

The lack of a functional *p21^{WAF1/CIP1}* gene ameliorates progression to chronic renal failure

JUDIT MEGYESI*, PETER M. PRICE*[†], ESTHER TAMAYO[‡], AND ROBERT L. SAFIRSTEIN*

*Department of Medicine, Division of Nephrology, University of Arkansas for Medical Sciences, Little Rock, AR 72205; and [‡]Department of Medicine, Division of Nephrology, University of Texas Medical Branch, Galveston, TX 77555-0562

Edited by Maurice B. Berg, National Institutes of Health, Bethesda, MD, and approved June 25, 1999 (received for review April 22, 1999)

ABSTRACT Partial renal ablation leads to progressive renal insufficiency and is a model of chronic renal failure from diverse causes. We find that mice develop functional and morphologic characteristics of chronic renal failure after partial renal ablation, including glomerular sclerosis, systemic hypertension, and reduced glomerular filtration. However, we now report that littermates with a homozygous deletion of the gene for the cyclin-dependent kinase inhibitor, *p21^{WAF1/CIP1}*, do not develop chronic renal failure after ablation. The markedly different reactions of the *p21*(+/+) and *p21*(-/-) animals was not because of differences in glomerular number or degree of renal growth but rather because of the presence or absence of a normal *p21* gene. Although the reaction to the stress of renal ablation is both hyperplastic and hypertrophic in the presence of a functional *p21* gene, it would appear that the absence of the *p21* gene may induce a more hyperplastic reaction because proliferating-cell nuclear antigen expression, a marker of cell-cycle progression, in the renal epithelium of the remnant kidney was more than five times greater in the *p21*(-/-) mice than in the *p21*(+/+) animals. Because *p21* is a potent inhibitor of the cell cycle, we speculate that *p21* regulates the balance between hyperplasia and hypertrophy after renal ablation. We propose that this change in response inhibits the development of chronic renal failure. These studies suggest that controlling *p21* function may ameliorate or even prevent progressive end-stage renal disease.

The removal of substantial amounts of renal tissue is followed by a progressive decline in renal function (1, 2). Glomerular hypertrophy occurs early in response to this ablation and is accompanied by short-term increases in glomerular filtration (3, 4). These structural and functional adaptations to loss of excretory function are thought to be maladaptive and to influence the progression to end-stage renal disease. Progression is initially seen as localized increases in mesangial matrix that then leads to global glomerular sclerosis and is usually associated with systemic hypertension, which has been speculated to accelerate its course. Although the early glomerular hypertrophy and hyperfunction, especially the glomerular hypertrophy that determines it, have been invoked as predeterminants of the later destructive effects of renal ablation, there is no established causal link between these events and the progressive nature of the renal disease.

Acute short-term stress in the kidney provokes molecular responses that involve the expression of several genes, including the cyclin-dependent kinase inhibitor *p21* (5). *p21* plays a critical role in processes by which nuclear events subsequent to environmental stress are regulated. It is induced to very high levels by oxidative stress (6) and DNA damage (7). The *p21* protein (8) acts as an inhibitor of cyclin-dependent kinase

activity (9) and effectively stops cell-cycle progression (8, 9). It is overexpressed in many cells undergoing senescence (10) or terminal differentiation (11, 12). The expression of *p21* after short-term chemotoxic renal stress is rapid, and that expression under these circumstances played a protective role (13). We speculated that chronic, long-term stress would provoke sustained expression of *p21* and that such expression could influence renal function and morphology. To test this hypothesis, we used renal ablation, a model of progressive renal insufficiency, as a chronic stress. Two groups of mice were compared: one in which the *p21* gene was deleted and their wild-type littermates. We report that in the absence of a functional *p21* gene, renal ablation did not result in progressive renal failure, which in the *p21*(+/+) mice included the development of glomerulosclerosis and systemic hypertension.

METHODS

Animal Preparation. Mice (strain 129/Sv) carrying a deletion of a large portion of the *p21* gene in which neither *p21* mRNA nor *p21* protein is expressed (14) were obtained from Philip Leder (Harvard Medical School, Boston). Mice homozygous for the *p21* deletion were selected from the offspring of heterozygous matings by using Southern blotting of tail DNA as described (14). Wild-type *p21*(+/+) littermates were used as controls for a normal *p21* gene. The animals were housed at the Animal Research Center at the University of Texas Medical Branch at Galveston. Food and water were supplied *ad libitum*. Body weights were determined at the start of the protocol, at the time of surgery, and at the time of sacrifice.

Renal ablation was created by two-step nephrectomy (15) by using 6- to 8-week-old male mice. At the first stage of the procedure, the right kidney was decapsulated, and the upper and lower poles were resected under anesthesia with pentobarbital sodium (50 mg/kg) i.p. Bleeding was prevented by using a thrombin solution (3,000 units/ml, 0.9% NaCl). One week later, a total left nephrectomy was performed under anesthesia as described above. Renal function, kidney morphology, morphometry, and mean arterial blood pressure were studied at various times thereafter.

Clearance and Direct Systolic Blood Pressure Measurements. Mice were anesthetized, as above, and placed on a heated surgical table to maintain body temperature between 37 and 38°C. Polyethylene catheters were placed in the trachea, bladder, both femoral arteries, and left jugular vein. The mean arterial blood pressure was obtained via the left femoral artery by using a strain-gauge transducer (Gould, Cleveland). The animals were infused with 0.9% sodium chloride solution via the left external jugular vein at a rate of 0.5% body weight per

The publication costs of this article were defrayed in part by page charge payment. This article must therefore be hereby marked "advertisement" in accordance with 18 U.S.C. §1734 solely to indicate this fact.

PNAS is available online at www.pnas.org.

This paper was submitted directly (Track II) to the *Proceedings* office. Abbreviations: PCNA, proliferating-cell nuclear antigen; GFR, glomerular filtration rate.

A Commentary on this article begins on page 10551.

[†]To whom reprint requests should be addressed. E-mail: PricePeterM@exchange.uams.edu.

Table 1. Physical parameters in untreated mice: Body weight, kidney weight, glomerular number, glomerular volume, and GFR

	Body weight, g	Kidney weight, mg/g body weight	Glomeruli per kidney, no.	Mean glomerular volume $\times 10^{-5}$, μm^3	C _{inulin} , ml/min
<i>p21</i> (+/+)	24.35 \pm 2.68	5.938 \pm 0.656	12,583 \pm 681	1.92 \pm 0.58	1.088 \pm 0.072
<i>p21</i> (-/-)	28.47 \pm 4.18	5.720 \pm 0.607	12,091 \pm 555	1.74 \pm 0.14	1.050 \pm 0.076
<i>P</i> value	<0.001	NS	NS	NS	NS

Values are means \pm SD. NS, not significant.

hour by using a constant-infusion syringe pump (model 355, Sage Instruments, Boston). The infusion solution contained enough [³H]methoxyinulin (American Radiolabeled Chemicals, St. Louis) to deliver 10 $\mu\text{Ci}/\text{hour}$. After a 60-minute equilibration period, urine was collected under mineral oil for three 30-minute clearance determinations. Blood was drawn in heparinized microhematocrit tubes from the right femoral artery at the beginning and end of the clearance period to determine hematocrit and ³H activity. ³H activity in urine and plasma was determined in a liquid scintillation counter (LKB Wallace 1211 RackBeta), and the glomerular filtration rate (GFR) was calculated (see below).

Kidney Morphology and Morphometry. At the time of sacrifice, kidney remnants were freed from the surrounding tissues, weighed, cut in half, fixed in 4% neutral buffered formaldehyde, and processed for light microscopy by paraffin embedding. Sections (5 μm) were stained with hematoxylin/eosin, periodic acid/Schiff reagent, or trichrome.

Morphological Studies. Three to five animals at various time points were used for morphological studies. By using periodic acid/Schiff reagent-stained sections, at least 300 glomeruli were evaluated by light microscopy. The percentage of each glomerulus exhibiting mesangial expansion or glomerulosclerosis was determined by point counting (4) at $\times 400$ by using an eyepiece reticle (SO75963, Nikon) Focal glomerulosclerosis was graded as to percent of glomerular area sclerotic by using the following criteria: minimal (1–25%), moderate (26–50%), and severe (51–84%). When $\geq 85\%$ of glomerular area was sclerotic, the glomerulus was classified as globally sclerotic.

Glomerular Morphometry. To determine glomerular hypertrophy, we measured mean glomerular volume (μm^3) based on point counting (16–18) according to the following formula:

$$\text{MGV} = 1.25 \left[\left(\frac{\text{antilog } \sum \log P}{n} \right) k^2 \right]^{3/2}$$

where *P* = number of points falling on each glomerular tuft profile, *k* = distance between the points in micrometers, and

n = number of glomeruli counted. Glomeruli showing global sclerosis were excluded.

Quantitation of Glomerular Numbers per Kidney. The number of glomeruli per kidney was determined by using the method described by MacKay *et al.* (19).

Immunohistochemistry. Proliferating-cell nuclear antigen (PCNA) was detected by using a mouse mAb (Santa Cruz Biotechnology) and the ABC Elite Vectastain kit (Vector Laboratories) according to manufacturers instructions.

In Situ Hybridization. *In situ* localization of *p21* mRNA on kidney sections was performed as described (5).

Calculations. GFR was calculated as $C_{\text{inulin}} (\text{ml}/\text{min}) = U/P [^3\text{H}] \times V_u (\text{ml}/\text{min})$. Percent nephrectomy was calculated as % nephrectomy = $(RK_{\text{removed}} + LK_{\text{adj}}) \times 100/2 \times LK_{\text{adj}}$, where RK_{removed} was the amount (mg) of the right kidney removed in the first operation and LK_{adj} was the weight (mg) of the left kidney removed in the second operation 7 days later, adjusted for hypertrophy between the first and second operation. The adjustment is calculated by multiplying the weight of the left kidney at the time of removal by the average kidney weight per body weight of untreated animals divided by the average kidney weight per body weight of day-7 left kidneys. Percent hypertrophy was calculated as % hypertrophy = $[(RK_{\text{final}} - RK_{\text{intact}})/RK_{\text{intact}}] \times 100$, where RK_{final} was the weight (mg) of right kidney at sacrifice, and RK_{intact} is $LK_{\text{adj}} - RK_{\text{removed}}$.

Statistical Analysis. Results are presented as mean \pm SE. Differences between means were evaluated by using Student's *t* test for unpaired data. *P* < 0.05 was considered statistically significant.

RESULTS

Body Weight and Renal Parameters Before Ablation. Body weight, kidney weight, glomerular number and volume, and renal function in untreated *p21*(+/+) and *p21*(-/-) mice are given in Table 1. There were no phenotypic differences between the two groups of mice, although the untreated *p21*(-/-) animals were about 15% (*P* < 0.001) larger than

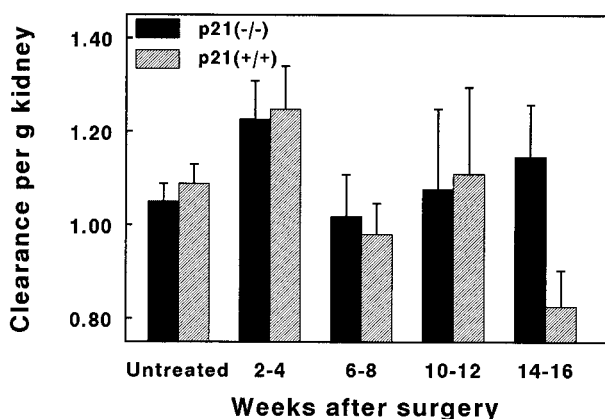


FIG. 1. Renal function after ablation. Clearance of inulin (ml per minute) was calculated per gram kidney in mice from both genotypes. Statistically significant differences were only noted between the two populations at 14–16 weeks after ablation (*P* = 0.04). Values represent mean \pm SE.

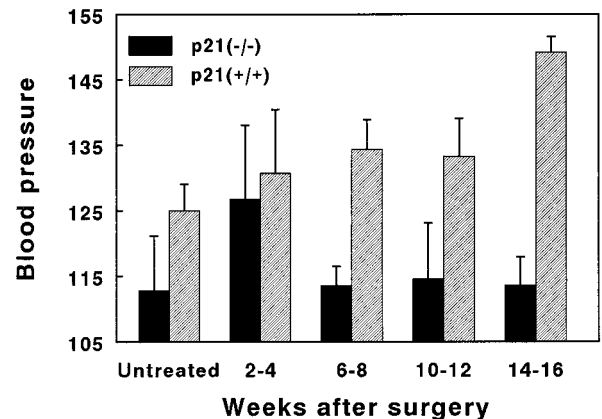


FIG. 2. Mean arterial pressure. Mean systolic blood pressure was obtained by catheterizing the left femoral artery. Statistically significant differences between the two populations was noted as early as 6–8 weeks after ablation (*P* = 0.005), which increased by 14–16 weeks after ablation (*P* = 0.00002). Values represent mean \pm SE.

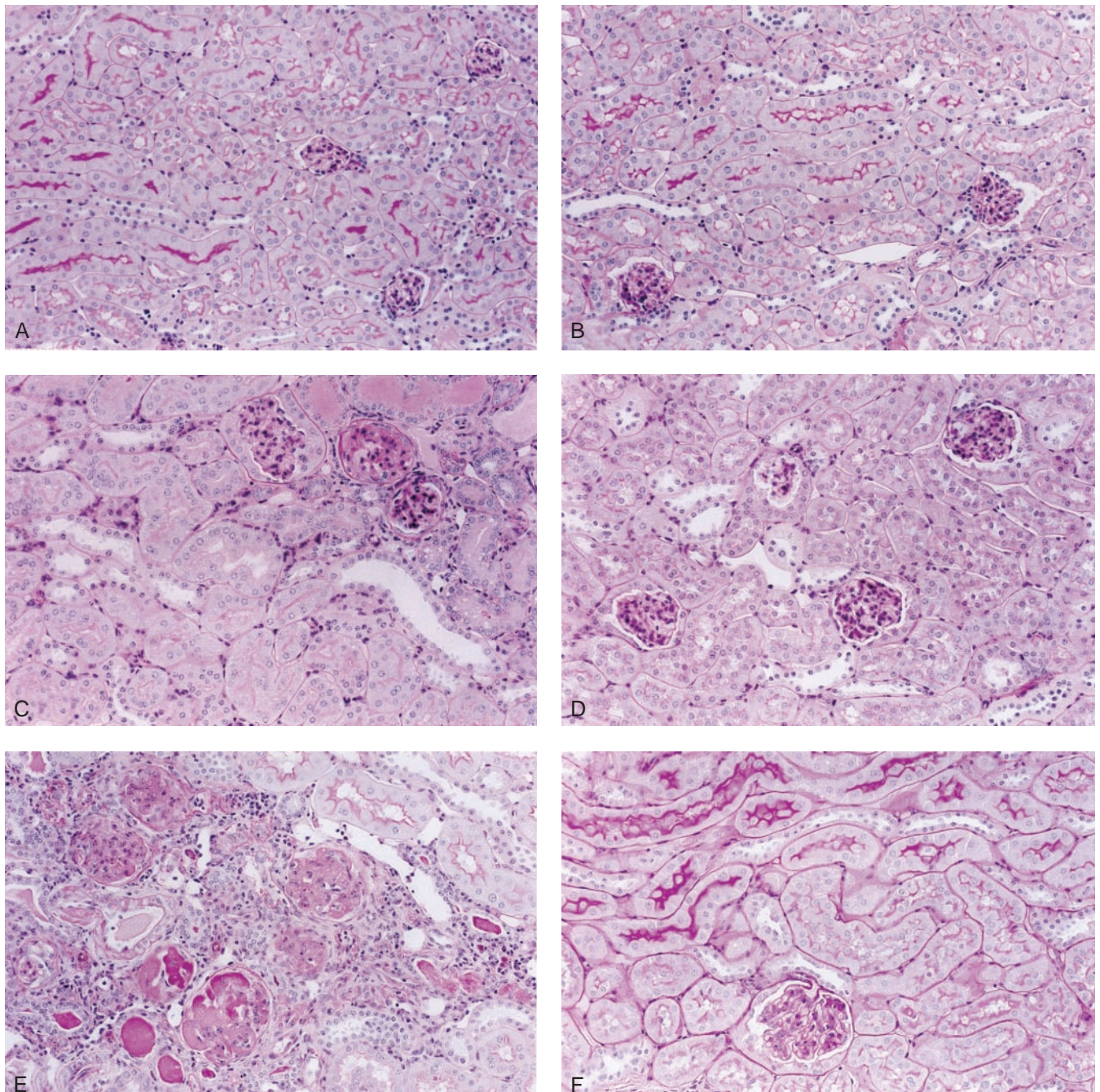


FIG. 3. Histologic changes in remnant kidney after ablation. Representative sections from either untreated (*A* and *B*), 8 weeks (*C* and *D*), 16 weeks (*E*), or 26 weeks (*F*) after ablation of wild-type (*A*, *C*, and *E*) or *p21*^{-/-} (*B*, *D*, and *F*) mice. Magnification, $\times 390$. Sections were stained with periodic acid/Schiff reagent.

those in the *p21*^{+/+} group. Size increases have also been reported in mice lacking the p27 cyclin-dependent kinase inhibitor genes (20–23). However, kidney weight per gram body weight, total glomerular number, and mean glomerular volume were not different between the two genotypes. Similarly, the two-kidney glomerular filtration rate, expressed as C_{inulin} of the untreated animals, were not different.

Body Weight, Degree of Ablation, Remnant Hypertrophy, and Mean Glomerular Volume After Ablation. Weight gain in renal ablated mice throughout the 14- to 16-week period of observation was not significantly different between the two groups, either in absolute terms (2.3 ± 0.8 g vs. 4.3 ± 1.1 g; $+/+$ vs. $-/-$ groups, respectively; $n = 11$ in each group) or

relative to initial body weight ($10.2 \pm 3.5\%$ vs. $15.9 \pm 4.3\%$; $+/+$ vs. $-/-$ groups, respectively). The degree of renal ablation was determined for each genotype. Approximately 2/3 of the normal renal mass was removed after the two operations, and there was no significant difference between the groups. The percent nephrectomy in the *p21*^{+/+} and *p21*^{-/-} groups was $68.8 \pm 3.6\%$ and $68.3 \pm 3.1\%$ ($P = 0.619$), respectively. Furthermore, the degree of hypertrophy and the mean glomerular volume after ablation (Table 2) were not significantly different between the groups.

Renal Function After Ablation. GFR increased to the same extent 2–4 weeks after ablation in both groups (Fig. 1). GFR was similar in both groups until the 14th–16th week after

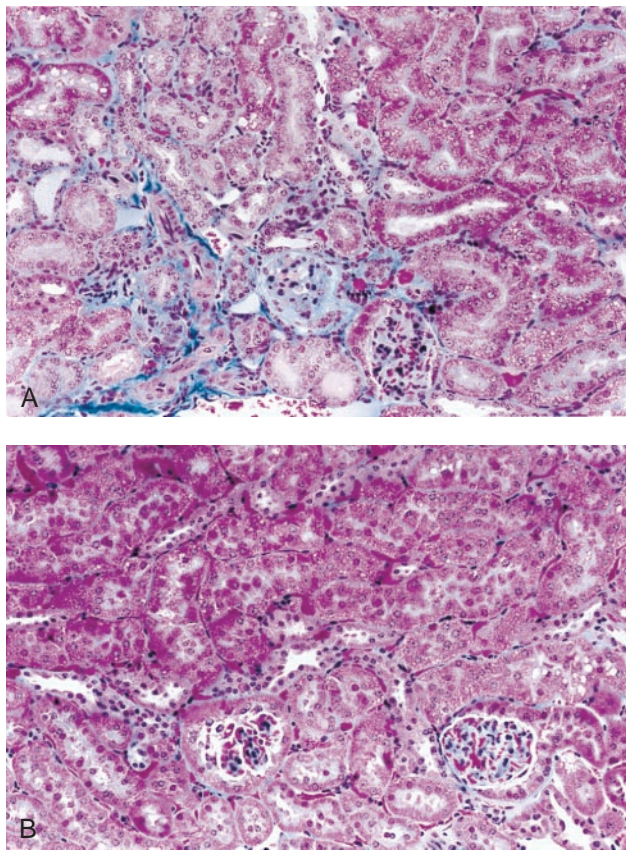


FIG. 4. Detection of interstitial fibrosis by using trichrome stain in remnant kidney after ablation. Representative sections from either 6 weeks (A) or 26 weeks (B) after ablation of wild-type (A) or *p21(-/-)* (B) mice. Magnification, $\times 390$.

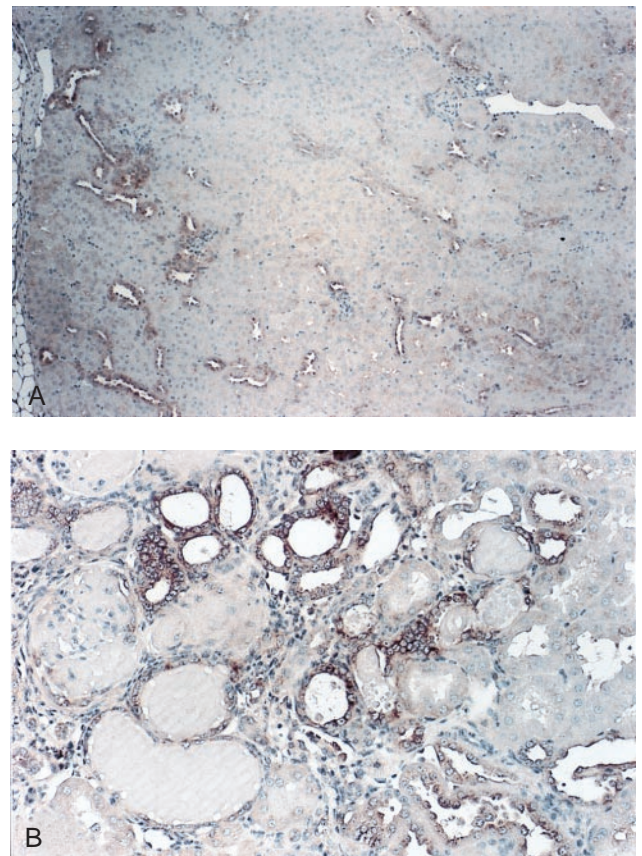


FIG. 5. *In situ* hybridization for localization of *p21* mRNA in remnant kidney cells after partial renal ablation. Hybridization of an antisense *p21* probe to RNA in cells of remnant kidney 4 weeks (A) and 14 weeks (B) after ablation. Magnification, $\times 390$.

ablation when it fell in the wild-type animals but remained unchanged from previous values in the *p21(-/-)* group. The GFR at this time point was significantly different between the two groups ($P < 0.05$).

Mean Arterial Pressure. Mean arterial pressure was not significantly different between the untreated groups of animals (Fig. 2). After partial renal ablation, arterial pressure increased initially in both groups of animals and increased further in the *p21(+/+)* mice so that by the 14th–16th week, the average mean systolic pressure reached 150.7 ± 6.7 mmHg (mean \pm SD). By contrast, mean systolic blood pressure in the *p21(-/-)* mice returned toward normal and remained there throughout the 16-week period of observation (113.8 ± 17.7 after 16 weeks versus 112.8 ± 16.7 in untreated mice).

Morphology. Light microscopic study revealed a marked difference of histologic changes between the two groups of mice. Representative micrographs are shown in Figs. 3 and 4; the changes were quantified in Table 3. Kidney sections from untreated mice were morphologically indistinguishable (Fig. 3 A and B). Mesangial expansion and mild focal glomerulosclerosis was observed in $\approx 70\%$ of glomeruli in the *p21(+/+)*

mice 4 weeks after ablation (Table 3). Beginning at 6–8 weeks, these mice developed severe focal and global glomerulosclerosis (Figs. 3 C vs. D and 4A, Table 3). All of the *p21(+/+)* mice studied developed glomerulosclerosis accompanied by interstitial fibrosis and round cell infiltration by 14–16 weeks postablation (Fig. 3E, Table 3). In contrast, *p21(-/-)* mice never developed glomerulosclerosis nor interstitial changes even 26 weeks after renal ablation (Figs. 3F and 4B), although mesangial expansion was seen occasionally.

The percentages of glomerulosclerosis in the *p21(+/+)* mice at various times after ablation are quantified in Table 3. It can be seen that they developed a progressive increase in glomerular sclerosis. The *p21(-/-)* mice do not develop glomerulosclerosis throughout the period of observation and were omitted from Table 3.

Expression of *p21* in the Remnant Kidney. *In situ* hybridization (Fig. 5) for *p21* mRNA identified the cells of the cortical thick ascending limbs and distal convoluted tubules as the principal site of *p21* expression 4 weeks after ablation (Fig. 5A). At later times, *p21* was also expressed in the epithelium of

Table 2. Percent hypertrophy and mean glomerular volume after renal ablation

Weeks	Hypertrophy			Mean glomerular volume		
	<i>p21(+/+)</i>	<i>p21(-/-)</i>	<i>t</i> test	<i>p21(+/+)</i>	<i>p21(-/-)</i>	<i>t</i> test
0	NA	NA	NA	1.92 ± 0.58	1.74 ± 0.14	NS
2–4	66.9 ± 28.6	83.9 ± 85.7	NS	1.93 ± 0.32	2.58 ± 0.71	NS
6–8	86.8 ± 41.5	138.5 ± 55.8	NS	2.71 ± 0.33	2.99 ± 0.34	NS
10–12	137.1 ± 88.7	141.4 ± 31.3	NS	3.52 ± 0.21	3.34 ± 0.37	NS
14–16	145.0 ± 37.0	135.9 ± 42.1	NS	2.87 ± 0.50	3.17 ± 0.38	NS

Values are mean \pm SD. NS, not significant; NA, not applicable.

Table 3. Development of glomerulosclerosis in *p21*(+/+) mice

Weeks	Glomerulosclerosis				
	None	Minimal	Moderate	Severe	Global
4	30.7 ± 0.9	65.8 ± 1.6	2.8 ± 1.7	0.8 ± 0.7	0
6–8	27.8 ± 5.1	41.0 ± 2.7	22.2 ± 3.5	4.9 ± 1.8	4.2 ± 3.5
10–12	15.3 ± 3.2	38.2 ± 7.8	25.2 ± 3.5	10.2 ± 3.3	11.1 ± 6.8
14–16	23.6 ± 2.5	22.4 ± 4.4	36.5 ± 4.1	9.5 ± 1.9	8.1 ± 3.9

Percent glomeruli in each category (±SE) as defined in *Materials and Methods*.

tubules (primarily dilated and collapsed) and glomeruli within or adjacent to sclerotic areas of the remnant kidney (Fig. 5B).

Cell Cycle Analysis. Nuclear PCNA, a marker for cells in the S phase of the cell cycle, was found in many cells of the remnant kidney in the *p21*(-/-) mice 2 weeks after surgery (Fig. 6A). The positive nuclei were primarily localized in the proximal convoluted tubules and occasionally in the glomeruli and distal convoluted tubules. By contrast, few cell nuclei were stained in the *p21*(+/+) remnant kidney (Fig. 6B). This difference in PCNA staining was quantified in nuclei from *p21*(-/-) mice (18.64 ± 0.73 per mm²) and *p21*(+/+) mice (3.50 ± 0.65 per mm²) and was highly significant ($P = 0.00006$). At later time points, PCNA was greatly diminished in both animals (data not shown).

DISCUSSION

These studies show that mice lacking a *p21* gene are resistant to the functional and morphologic consequences of partial renal ablation. Not only is the resistance manifested locally in

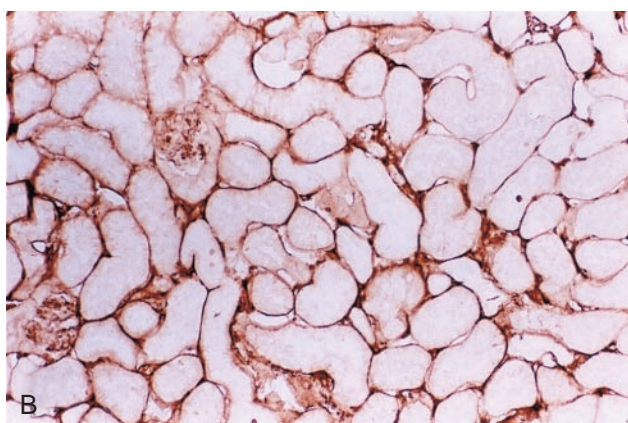
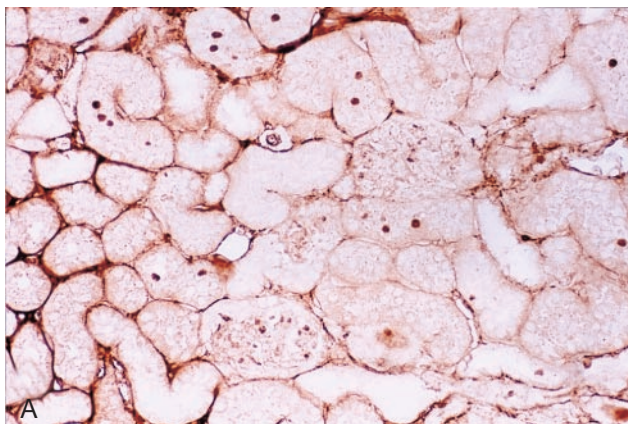


FIG. 6. Cell cycle analysis in remnant kidney cells after partial renal ablation. Immunodetection of nuclear PCNA localization 2 weeks after ablation in kidney sections from *p21*(-/-) (A) and wild-type (B) mice. Magnification, ×390.

the surgically impaired remnant organ, but it is also evident systemically in the lack of increased arterial pressure. In considering the reasons for this resistance, we evaluated several parameters speculated to be early determinants of the long-term outcome of renal ablation. Severe protein restriction can partially ameliorate the development of glomerulosclerosis after partial renal ablation (24). However, weight gains in the two groups of animals were not significantly different, and the *p21*(-/-) mice even experienced slightly elevated gains, both relative and absolute. Reduced glomerular number is thought to be an etiologic link in the progressive nature of renal disease (25, 26). The *p21*(+/+) and *p21*(-/-) animals had similar numbers of glomeruli at the outset of the experiments (Table 1), and the degree of renal ablation was the same for each group. Thus, the loss of renal excretory function was equally applied to both groups. The increase in glomerular filtration that occurs in response to renal ablation, also thought to be an early determinant of the progression (4), occurred to the same extent in the *p21*(-/-) animals as it did in the wild type (Fig. 1). Glomerular hypertrophy, which has an independent role in the progression of renal ablation models of experimental renal disease (27), occurred to the same extent in both groups as well (Table 2).

Taken together, these observations are most consistent with a critical role of the *p21* gene product in the functional and morphologic consequences subsequent to the stress of renal ablation, including the development of glomerular sclerosis and hypertension. The data also show that hypertension does not develop without the development of renal damage. We speculate that this resistance is critically linked to the prominent role the *p21* protein plays in regulating the cell cycle. The growth of the kidney after renal ablation is a consequence of hyperplasia and hypertrophy of the glomerular and epithelial compartments of the kidney (28, 29). However, hypertrophy may be, in the long term, a maladaptive response to the loss of functional renal tissue (4, 27, 30). In the absence of the *p21* gene, the growth response of the kidney after partial ablation is relatively more hyperplastic than hypertrophic. Consistent with this notion is a >5-fold increase in PCNA protein expression in *p21*(-/-) animals compared with the wild-type animals undergoing the response to renal ablation. By achieving growth after renal ablation by increasing the relative contribution of hyperplasia, the workload of the kidney is better accommodated. This proposal, first expressed by Goss (31), assumes that when an organ accommodates increases in work by hypertrophy rather than hyperplasia, it is at a serious physiologic disadvantage and is more likely to undergo regression of structure and function. Confirmation of this hypothesis must await a detailed description of the differences in the balance between hypertrophy and hyperplasia in the two groups of mice and, more specifically, the sites at which these differences are apparent. Regardless of its precise role, it is clear that *p21* is a critical sensor of the stress of renal mass reduction. This model should be useful in identifying the mechanism of how this response to renal ablation is maladaptive. The studies also suggest that manipulation of *p21* gene expression could be a target for the treatment of progressive renal failure.

We thank Philip Leder (Harvard Medical School) for providing several heterozygous mice carrying the *p21* gene deletion and for providing a probe for screening and Bert Vogelstein (Johns Hopkins Oncology Center) for cloned mouse *p21* cDNA. We also thank Thomas Andreoli (University of Arkansas) for his comments on the manuscript. The authors are supported in part by a grant from the National Institutes of Health (R01 DK54471).

1. Chanutin, A. & Ferris, E. B., Jr. (1932) *Arch. Intern. Med.* **49**, 767–787.
2. Morrison, A. B. (1962) *Lab Invest.* **11**, 321–332.
3. Faraj, A. H. & Morley, A. R. (1992) *APMIS* **100**, 1097–1105.

4. Daniels, B. S. & Hostetter, T. H. (1990) *Am. J. Physiol.* **258**, F1409–F1416.
5. Megyesi, J., Udvarhelyi, N., Safirstein, R. L. & Price, P. M. (1996) *Am. J. Physiol.* **271**, F1211–F1216.
6. Gorospe, M., Martindale, J. L., Sheikh, M. S., Fornace, A. J., Jr. & Holbrook, N. J. (1996) *Mol. Cell. Differ.* **4**, 47–65.
7. El-Deiry, W. S., Tokino, T., Velculescu, V. E., Levy, D. B., Parsons, R., Trent, J. M., Lin, D., Mercer, W. E., Kinzler, K. W. & Vogelstein, B. (1993) *Cell* **75**, 817–825.
8. Xiong, Y., Zhang, H. & Beach, D. (1992) *Cell* **71**, 505–514.
9. Harper, J. W., Adami, G. R., Wei, N., Keyomarsi, K. & Elledge, S. J. (1993) *Cell* **75**, 805–816.
10. Noda, A., Ning, Y., Venable, S. F., Pereira-Smith, O. M. & Smith, J. R. (1994) *Exp. Cell Res.* **211**, 90–98.
11. Steinman, R. A., Hoffman, B., Iro, A., Guillouf, C., Liebermann, D. A. & el-Houseini, M. E. (1994) *Oncogene* **9**, 3389–3396.
12. Jiang H., Lin, J., Su, Z. Z., Collart, F. R., Huberman, E. & Fisher, P. B. (1994) *Oncogene* **9**, 3397–3406.
13. Megyesi, J., Safirstein, R. L. & Price, P. M. (1997) *J. Clin. Invest.* **101**, 777–782.
14. Deng, C., Zhang, P., Harper, J. W., Elledge, S. J. & Leder, P. (1995) *Cell* **82**, 675–684.
15. Hamamori, Y., Samal, B., Tian, J. & Kedes, L. (1995) *J. Clin. Invest.* **95**, 1808–1813.
16. Nath, K. A. & Salahudeen, A. K. (1990) *J. Clin. Invest.* **86**, 1179–1192.
17. Hirose, K., Østerby, R., Nozawa, M. & Gundersen, H. J. G. (1982) *Kidney Int.* **21**, 689–695.
18. Bilous, R. W., Mauer, S. M., Sutherland, D. E. R. & Steffes, M. W. (1989) *Diabetes* **38**, 1142–1147.
19. MacKay, K., Striker, L. J., Pinkert, C. A., Brinster, R. L. & Striker, G. E. (1987) *Kidney Int.* **32**, 827–837.
20. Nakayama, K., Ishida, N., Shirane, M., Inomata, A., Inoue, T., Shishido, N., Horii, I., Loh, D. Y. & Nakayama, K.-i. (1996) *Cell* **85**, 707–720.
21. Kiyokawa, H., Kineman, R. D., Manova-Todorova, K. O., Soares, V. C., Hoffman, E. S., Ono, M., Khanam, D., Hayday, A. C., Frohman, L. A. & Koff, A. (1996) *Cell* **85**, 721–732.
22. Fero, M. L., Rivkin, M., Tasch, M., Porter, P., Carow, C. E., Firpo, E., Polyak, K., Tsai, L.-H., Broudy, V., Perlmutter, R. M., *et al.* (1996) *Cell* **85**, 733–744.
23. Franklin, D. S., Godfrey, V. L., Lee, H., Kovalev, G. I., Schoonhoven, R., Chen-Kiang, S., Su, L. & Xiong, Y. (1998) *Genes Dev.* **12**, 2899–2911.
24. Brenner, B. M., Meyer, T. W. & Hostetter, T. H. (1982). *N. Engl. J. Med.* **307**, 652–660.
25. Brenner, B. M., Garcia, D. L. & Anderson, S. (1988) *Am. J. Hypertens.* **1**, 335–347.
26. Fetterman, G. H. & Habib, R. (1969) *Am. J. Clin. Path.* **52**, 199–207.
27. Yoshida, Y., Fogo, A. & Ichikawa, I. (1989) *Kidney Int.* **35**, 654–660.
28. Terzi, F., Ticozzi, C., Burtin, M., Motel, V., Beaufils, H., Laouari, D., Assael, B. M. & Kleinknecht, C. (1995) *Am. J. Physiol.* **268**, F793–F801.
29. Floege, J., Burns, M. W., Alpers, C. E., Yoshimura, A., Pritzl, P., Gordon, K., Seifert, R. A., Bowen-Pope, D. F., Couser, W. G. & Johnson, R. J. (1992) *Kidney Int.* **41**, 297–309.
30. Fries, J. W. U., Sandstrom, D. J., Meyer, T. W. & Rennke, H. G. (1989) *Lab. Invest.* **60**, 205–218.
31. Goss, R. J. (1966). *Science* **153**, 1615–1620.